Genotypic variations and interspecific interactions modify gene expression and biofilm formation of Xanthomonas retroflexus

Samuel Jacquiod, Nanna Mee Coops Olsen, Manuel Blouin, Henriette Lyng Røder, Mette Burmølle

Received: 10 May 2023 | Accepted: 8 August 2023

DOI: 10.1111/1462-2920.16503

RESEARCH ARTICLE

ENVIRONMENTAL MICROBIOLOGY Applied Microbiology International

Genotypic variations and interspecific interactions modify gene expression and biofilm formation of *Xanthomonas retroflexus*

Samuel Jacquiod[1] | **Nanna Mee Coops Olsen**[2] | **Manuel Blouin**[1] | **Henriette Lyng Røder**[2,3] | **Mette Burmølle**[2]

[1]Agroécologie, INRAE, Institut Agro Dijon, Université de Bourgogne, University Bourgogne Franche-Comté, Dijon, France

[2]Section of Microbiology, Department of Biology, University of Copenhagen, Copenhagen, Denmark

[3]Section of Microbiology and Fermentation, Department of Food Science, University of Copenhagen, Copenhagen, Denmark

Correspondence
Samuel Jacquiod, Agroécologie, INRAE, Institut Agro Dijon, Université de Bourgogne, University Bourgogne Franche-Comté, F-21000 Dijon, France.
Email: samuel.jacquiod@u-bourgogne.fr

Mette Burmølle, Section of Microbiology, Department of Biology, University of Copenhagen, Copenhagen, Denmark.
Email: burmolle@bio.ku.dk

Funding information
Novo Nordisk Fonden, Grant/Award Number: 27620; I-SITE Junior Fellowship BFC, Grant/Award Number: RA19028.AEC.IS; Villum Fonden, Grant/Award Number: 10098/35906/34434

Abstract

Multispecies biofilms are important models for studying the evolution of microbial interactions. Co-cultivation of *Xanthomonas retroflexus* (XR) and *Paenibacillus amylolyticus* (PA) systemically leads to the appearance of an XR wrinkled mutant (XRW), increasing biofilm production. The nature of this new interaction and the role of each partner remain unclear. We tested the involvement of secreted molecular cues in this interaction by exposing XR and XRW to PA or its supernatant and analysing the response using RNA-seq, colony-forming unit (CFU) estimates, biofilm quantification, and microscopy. Compared to wild type, the mutations in XRW altered its gene expression and increased its CFU number. These changes matched the reported effects for one of the mutated genes: a response regulator part of a two-component system involved in environmental sensing. When XRW was co-cultured with PA or its supernatant, the mutations effects on XRW gene expression were masked, except for genes involved in sedentary lifestyle, being consistent with the higher biofilm production. It appears that the higher biofilm production was the result of the interaction between the genetic context (mutations) and the biotic environment (PA signals). Regulatory genes involved in environmental sensing need to be considered to shed further light on microbial interactions.

INTRODUCTION

With their short life cycles and strong capacity for adaptation, microorganisms are useful models for studying selection and evolution (McDonald, 2019), including the evolution of interspecific interactions, which has historically been challenging (Futuyma, 2010; Thompson, 1999). Previous efforts in this area have utilised both modelling (Williams & Lenton, 2007) and experimental approaches (Fiegna et al., 2015; Scheuerl et al., 2020), but it remains difficult to decode the interplay between the genetic and environmental determinants that shape the evolution of interactions (Hansen et al., 2007; Liu et al., 2019). Microorganisms adapt quickly to changes in environmental conditions, especially in laboratory settings (Lenski, 2017; Røder et al., 2018). Of the adaptive mechanisms at play, genetic variations arising from mutations are crucial, as they may have consequences not only for the mutated organisms themselves (Lenski, 2017), but also for other organisms that may interact with the mutants. A notable example of this are mutations that induce higher biofilm production (Hansen et al., 2007; Røder et al., 2018).

Samuel Jacquiod and Nanna Mee Coops Olsen shared first authorship.

Biofilms play an important role in the ecology and evolution of microbial multispecies assemblages; they represent well-delineated environments with high cell densities that support strong biotic interactions compared to planktonic environments (Røder et al., 2016). In addition, as they represent the dominant form in which bacteria are found in the environment (Bar-On & Milo, 2019; Flemming et al., 2016), biofilms are suspected to play a major role in microbial adaptation and evolution (Hansen et al., 2007). Living and interacting in biofilms provides a whole set of advantages that can improve microbial species' fitness depending on the context, such as the degradation of complex nutrients (Drescher et al., 2014; Nasipuri et al., 2020), stress tolerance (Lee et al., 2014; Yang et al., 2021), predator protection (Raghupathi et al., 2018) and even increased biofilm production itself (Liu et al., 2019; Madsen et al., 2016; Ren et al., 2015).

As an example, a remarkable interaction was described between two soil bacterial strains, *Xanthomonas retroflexus* (XR) and *Paenibacillus amylolyticus* (PA), which were co-isolated from the same micro-habitat (Ren et al., 2014). These two strains were previously shown to interact and influence eachother when grown together (e.g., pH neutralisation and metabolic interactions, Herschend et al., 2017, 2018). Furthermore, co-culture of these two strains resulted in enhanced biomass formation through increased biofilm production (Hansen et al., 2017). Furthermore, the effect of this interaction was boosted significantly by the appearance of an XR variant with a wrinkled-colony and less motile phenotype (XRW), which demonstrated improved biofilm formation during co-cultivation with PA (Røder et al., 2018). Such wrinkled mutants are commonly observed under lab settings (Boles et al., 2004; Poltak & Cooper, 2011), and their appearance is likely linked to changes in environmental conditions (e.g., accessibility to nutrients and oxygen Røder et al., 2019). However, the occurrence and abundance of such variants also appears to be influenced by biotic factors, as the wrinkled mutants were systematically observed in all XR–PA co-cultures (100% of tested wells), while they were detected only in some XR mono-cultures (72% of tested wells, Røder et al., 2018). This finding suggested the influence of a real but as-yet unknown, biotic interaction between these two species (Røder et al., 2018). Such 'wrinkled' or 'rugose' microbial phenotypes are known to affect biofilm functioning (Richter et al., 2018; Shi et al., 2013; Udall et al., 2015) and are thus keystone genotypes for understanding microbial interactions (Røder et al., 2018) and biofilm production (Malone et al., 2007; Spiers et al., 2003; Spiers & Rainey, 2005). Among the XRW variants isolated in earlier work, one was particularly efficient in producing biofilm when PA was present (Røder et al., 2018). This XRW variant featured two mutations in distinct coding DNA sequences (CDSs) that are apparently involved in cellulose biosynthesis (CDS_331: bacterial cellulose synthesis protein E [BcsE], closest homologue in *Salmonella enterica*) and cyclic di-guanosine 5-monophosphate (c-di-GMP) secondary messenger regulation (CDS_2260: response regulator, closest homologue in *Stenotrophomonas* spp.), respectively. The mutation in the response regulator seemed particularly important, as it was systematically found in all XRW variant tested, and CDS_2260 knockout mutants no longer showed wrinkled colonies (Røder et al., 2018). These two genes are known to be important for the regulation and production of biofilms in other species (Barnhart et al., 2013; Fang et al., 2014; Madsen et al., 2018; Paul et al., 2004; Valentini & Filloux, 2016), in conjunction with c-di-GMP, whose increased concentration in cells is known to be linked with sedentary lifestyle and biofilm formation (Kumari et al., 2022). Indeed, previous work on *Pseudomonas fluorescens SBW25* wrinkled genotypes have revealed the joint importance of response regulators involved in c-di-GMP synthesis and the bacterial cellulose synthesis pathways in biofilm formation (Malone et al., 2007; Spiers et al., 2003; Spiers & Rainey, 2005). However, the functional consequences of these mutations and their dependency on the environmental presence of PA have not yet been investigated. The aim of the current study was to determine if PA plays a direct role in biofilm synthesis as a producer itself, or instead acts indirectly by producing molecular signals that trigger more biofilm production by XRW. We thus decided to test the hypothesis that the enhanced biofilm production induced by the XRW–PA interaction emerges as a result of an interaction between the genetic background (XRW mutations) and the biotic environmental context (direct via presence of PA or indirect via signals emitted by PA).

To achieve this goal, we compared the XR wild type with the XRW variant featuring the mutations in BcsE and the response regulator in different biofilm contexts: (i) cultured alone (mono-cultures: XR or XRW), (ii) cultured with PA (co-cultures: XR-PA or XRW-PA), and, for the first time, (iii) cultured in the presence of PA supernatant (SN cultures: XR–SN or XRW–SN). With the mono-cultures, we aimed to determine the direct consequences of the mutations on XR and have a baseline for the characterisation of the effects of the biotic interaction in the co-cultures. The supernatant cultures were designed to reveal the nature of the interaction between PA and XR or XRW, which is suspected to occur via remote activation by molecular cues. To obtain the most comprehensive view of this biofilm model, we used an approach that integrated an in-depth bioinformatic analysis of the mutated peptides with total gene expression profiling (mRNA-seq) in order to gain insights into the consequences of the mutations in the different environmental contexts (mono-cultures, co-cultures and supernatants). These new analyses were complemented by fitness

estimations of each species (assessments of colony-forming units [CFUs]) from biofilms, biofilm quantification (crystal violet [CV] staining) and direct observations (scanning electron microscopy [SEM]). Our results revealed the crucial role of PA in modulating the effects of the mutations in XRW via secreted molecular signals. PA supernatant masked the effects of the mutations, resulting in the altered expression of a specific set of genes in XRW that are involved in sedentary lifestyle, which was consistent with the higher biofilm production observed.

EXPERIMENTAL PROCEDURES

Bioinformatic analysis of the two mutated peptides

The wild type and mutated peptide sequences predicted from CDS_331 and CDS_2260 of XR isolate 3 (European Nucleotide Archive [ENA]; PRJEB18431) were analysed using the approach described in Jacquiod et al. (2014). Sequences were obtained from the Rapid Annotation using Subsystem Technology database (RAST; Overbeek et al., 2014). We searched for protein domains using domain-enhanced lookup time accelerated BLAST (DELTA-BLAST; Boratyn et al., 2012), and for signal peptides using the Signal IP tool, v.5.0 (Nielsen, 2017). Protein domains involved in modulation of the c-di-GMP secondary messenger were analysed using a custom model for activity prediction (Madsen et al., 2018).

Strains and growth conditions

XR and PA were originally isolated from the same soil sample (Ren et al., 2014). The XR and PA genomes are accessible in the ENA (XR: PRJEB18431; PA: PRJEB15262). The XRW variant was isolated and sequenced in a previous study (originally named XR-Wa; Røder et al., 2018). Strains were kept in glycerol stocks (−80°C) and streaked onto Tryptic soy broth plates (TSB; 17 g of pancreatic digest of casein, 3 g of digest of soybean meal, 5 g of sodium chloride, 2.5 g of dextrose, 2.5 g of dibasic potassium phosphate in 1 L distilled water, pH 7.3; Sigma Aldrich, Germany) with agar (14 g/L, Sigma Aldrich, Germany) and incubated at 24°C for 48–72 h.

Biofilm production and supernatant preparation

Solid–liquid interface biofilms from batch cultures in microtiter plates were quantified using CV staining (O'Toole, 2011). Overnight strain cultures were re-inoculated and grown to the exponential phase (TSB, 24°C). Cells were washed three times, their concentration was adjusted based on optical density (OD) (TSB, $OD_{600} = 0.1$), and they were used to inoculate 96-well microtiter plates (Merck, cat. 655180, 150 μL/well). For the co-culture experiment, strains were inoculated at equal ratios based on OD_{600}. In using similar values of OD_{600} at inoculation, our intent was to provide the two species with equal access to the available surface, as the larger PA cells occupy a bigger volume and surface area. For the supernatant treatment, a single PA colony was grown in 5 mL of TSB for 20 h, then its supernatant was retrieved by filtering (0.2-μm PES filter, Fisher Scientific, cat. 15206869) and mixed 1:1 with pelleted and freshly resuspended XR or XRW cells (in TSB, $OD_{600} = 0.2$). Plates were incubated with shaking (150 rpm, 24°C, 24 h). Biofilms that formed in wells were washed (0.2% w/v NaCl, twice) and stained (1% w/v CV, 20 min). The residual biomass was washed (PBS, five times) and de-stained (96% v/v ethanol), and the absorbance was measured (595 nm, ELX 808IU Absorbance Microplate Reader, BioTek Instruments, Winooski, VT). The experiment was repeated on three different days using technical replicates ($N = 4$). Technical replicates were averaged before analysis.

Sampling for RNA sequencing and CFU counts from biofilms

CFU counts and samples for RNA sequencing were obtained from biofilms with an adjusted version of the preceding protocol (Biofilm production and supernatant preparation section). Biofilm quantification and CFU counts could not be performed simultaneously due to the destructive nature of CV quantification. For this reason, CFU counts were used as a proxy measurement of fitness in the biofilm environment. OD-adjusted cultures were inoculated into 24-well plates (Merck, cat. 662160) for all treatments as described above (1 mL/well, 24°C, 24 h, no shaking). For each well, the supernatant was removed and the entire biofilm structure (including top pellicle, well sides and bottom) was collected. Biofilm samples were re-suspended in 600 μL of RNA*later* (ThermoFisher, cat. AM7020) in 2-mL Eppendorf tubes and centrifuged (7000 rcf, 5 min). We then added 1 mL of fresh RNA*later* to each tube and stored them at −80°C. For each of the three treatments, five biological replicates were produced for XR ($N = 15$) and XRW ($N = 15$). To obtain CFU counts, the same assay was performed but, after supernatant removal, 600 μL of PBS were added to each well instead of RNA*later*. Samples were thoroughly vortexed and pipette-mixed to ensure complete dispersion of the biofilm. Serial dilutions (0.9% w/v NaCl) were plated on Tryptic soy agar plates with Congo red (40 μg/mL of Congo red, 20 μg/mL of Coomassie brilliant blue G250), and incubated (72 h,

24°C). Colony differentiation and counting were then performed based on morphology. The experiment was repeated on three different days using technical replicates ($N = 2$). Technical replicates were averaged before analysis.

RNA extraction, library preparation, and sequencing

Samples were shipped to the Beijing Genomics Institute (BGI, https://www.bgi.com/us/sequencing-services/dna-sequencing/), where RNA extraction and sequencing were performed following their procedures. Cells were disrupted (NucleoSpin Bead tubes, $Ø = 0.6$–0.8 mm, RLT buffer, full speed, 4 min, room temperature [RT]) and centrifuged (≥15,000 rpm, 2 min), and supernatants were transferred into RNase-free tubes. One volume of 70% v/v ethanol was added to the lysates and pipette-mixed. For each sample, a 700-μL aliquot was loaded onto an RNeasy spin column. Total RNA was purified and eluted from columns using the RNeasy Mini kit (Qiagen), and ribosomal RNA was removed using the Ribo-Zero rRNA Depletion kit (Qiagen). Reverse transcription was performed using random N6 primers, followed by end repair, A-tailing and adaptor ligation, to obtain complementary DNA (cDNA). cDNA was subjected to PCR amplification, followed by single-strand separation, cyclization and DNA nanoball synthesis. Sequencing was performed on the BGISEQ-500 platform and generated 50-bp single-end reads.

Transcriptomics analysis

For each sample, more than 14 million clean reads were generated that met the following thresholds: Q20 > 96% (% nucleotides with quality >20) and final rRNA content <1% ('*SortMeRNA*' v.2.0; Kopylova et al., 2012). Libraries were mapped to concatenated XR and PA genomes ('*Bowtie2*' v.2.2.3; Langmead & Salzberg, 2012), using predicted CDSs from RAST, the SEED subsystem and FIGfams database (XR Gene ID: 6666666.163022, 4158 CDSs; PA Gene ID: 6666666.122687, 6416 CDSs). For XR, 94.1%–97.8% of the genome was mapped, and 79.7%–89.8% for PA (Table S6). Sequence alignment maps were aligned with genomic features to yield contingency matrices using *featureCounts* ('*Rsubreads*'; Liao et al., 2014). Annotation and count tables are available in Supporting Data 4.

Scanning electron microscopy

For each treatment, SEM imaging was performed on cultures that had been prepared using a standardised growth procedure. Solid–liquid interface biofilms were formed on round cover slips submerged in liquid growth medium in 24-well plates in static conditions (2 mL of TSB, 24 h, RT, round coverslips Ø12 mm) and fixed overnight (RT, 2% of glutaraldehyde w/v in 0.1 M sodium cacodylate), with an extra incubation for lipid fixation (RT 1% of OsO_4 in 0.1 M sodium cacodylate). Biofilms were dehydrated with ascending concentrations of ethanol (from 50% v/v to 100%) and subjected to critical point drying with carbon dioxide. Samples were mounted on aluminium holders, sputtered with 20 nm of palladium/gold, and examined by SEM (Philips/FEI XL 30 FESEM, Everhart-Tornley secondary electron detector, Core Facility for Integrated Microscopy, Faculty of Health and Medical Sciences, University of Copenhagen). For the sake of reproducibility, several images were acquired for each treatment (Supporting Data 2).

Statistical analysis

Analyses were conducted with '*Rgui*' software (v.4.0.4; R Core Team, 2020). Depending on the normality of the data, CFU and biofilm data were analysed using either Analysis of Variance (ANOVA) with a post hoc Tukey's honest significant difference test (HSD, $p < 0.05$) or a Kruskal–Wallis test with *p*-values adjusted based on the false discovery rate (FDR, $p < 0.05$) with the '*agricolae*' package (de Mendiburu & Yaseen, 2020). The transcriptomic contingency tables were analysed with the '*vegan*' package (Oksanen et al., 2020). Differentially expressed genes (DEGs) were identified with a quasi-likelihood *F*-test under negative binomial distributions and generalised linear models using the '*edgeR*' package (Robinson et al., 2010). Clusters of orthologous groups of proteins predicted from DEGs was performed from RAST GTF files and online genome annotation submissions by *eggNOG-mapper* v2 v.4.5.1 (Huerta-Cepas et al., 2016).

RESULTS

Sequence analysis of the mutated CDSs

First, we thoroughly investigated the mutated peptide sequences to identify potential functional changes that could explain the increase in biofilm production compared to the wild type. Protein domain scans were performed using DELTA-BLAST. CDS_331 is part of a bacterial cellulose synthesis operon of nine genes (Figure 1A), which were all expressed in all our treatments (Figure S1). The predicted CDS_331 peptide had a significant match with the BcsE from *Salmonella enterica* (cover = 98%, sequence identity = 28%, *E*-value = 2.2×10^{-91}). This protein featured a

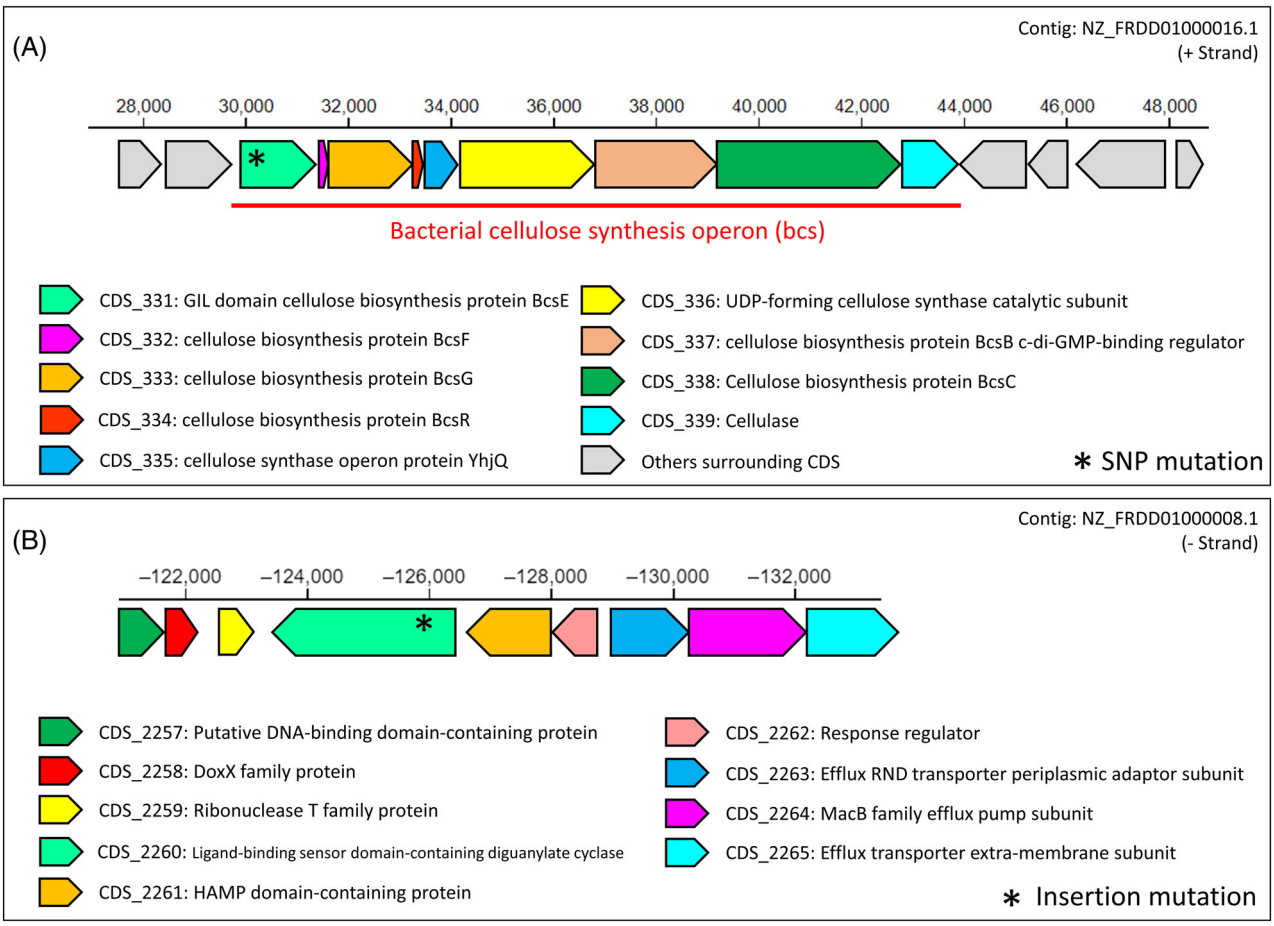

FIGURE 1 Genetic context of the two mutated genes in *Xanthomonas retroflexus* genome (refseq: NZ_FRDD01000031). (A) Genetic context of CDS_331 encoding the bacterial cellulose synthesis protein E (BcsE) protein, which is part of a bacterial cellulose synthesis operon of nine genes. A single-nucleotide polymorphism mutation occurred in the 'GIL' domain involved in cyclic di-guanosine 5-monophosphate (c-di-GMP) binding (see Supporting Data 1). (B) Genetic context of CDS_2260 encoding a periplasmic ligand-binding sensor domain-containing diguanylate cyclase, which is positioned next to gene encoding peptides with partner functions involved in sensors or signal transmitters (CDS_2261 HAMP and CDA-2260 response regulator). An insertion mutation occurred in the 'GGDEF' domain involved in c-di-GMP synthesis (see Supporting Data 1). CDS, coding DNA sequences.

cellulose biosynthesis protein GGDEF I-site-like domain ('CBP_GIL' domain) that, when activated by c-di-GMP at its two 'RXGD' binding sites, plays a role in increasing cellulose production (Fang et al., 2014). No signal peptide was detected, indicating probable cytoplasmic location. The mutation caused a single nucleotide polymorphism inside the 'CBP_GIL' domain, substituting a glutamic acid residue (E) with a lysine (K) (Supporting Data 1). CDS_2260 is located close to genes involved in signal transduction and response regulation (Figure 1B). The peptide matched with a ligand-binding sensor domain-containing diguanylate cyclase from *Stenotrophomonas* spp. (cover = 100%, identity = 99.6%, *E*-value = 8.18×10^{-70}), whose species members are known to produce biofilm (Cierra et al., 2022). The scanning revealed the presence of multiple domains (Supporting Data 1), including: (i) a periplasmic ligand-binding sensor domain involved in signal transduction mechanisms, (ii) a 'Y_Y_Y' domain of unknown function but typically found in at the end of the beta propellers in a family of two component regulators and (iii) a 'GGDEF' domain involved in synthesis of the c-di-GMP secondary messenger (c-di-GMP cyclase), sharing similarities with the 'PleD superfamily' domain characterised in the *Alphaproteobacterium Caulobacter crescentus* (Aldridge et al., 2003). Our custom pipeline for c-di-GMP domain prediction detected two 'EAL' domains involved in c-di-GMP degradation (c-di-GMP phosphodiesterase, Supporting Data 1), of which one contained the required accessory residues for full activity (Madsen et al., 2018). A signal peptide was detected in the N-terminal region, indicating probable transport to the membrane environment. The mutation in the CDS_2260 peptide caused the insertion of an additional 'EAL' domain at the beginning of the 'GGDEF domain' but away from active residues.

Microscopy observations, biofilm production and fitness estimation

We used SEM (Supporting Data 2) to visualise the biofilms of the mono-cultures (Figure 2A,B) and co-cultures (Figure 2C,D). XR cells were estimated to be 573 ± 21 nm in length and 231 ± 5 nm in diameter. In mono-cultures, XR had fewer attached cells and cell aggregates (Figure 2A), while, under similar conditions, XRW colonisation of the same surface was more pronounced, with visually higher cell numbers (sometimes forming long chains; Figure S2A) and large cell aggregates (Figure 2B). PA cells were estimated to be 2004 ± 57 nm in length and 555 ± 8 nm in diameter, making them larger than XR cells. Co-culturing with PA completely changed the biofilm morphology. Cells of PA attached together in long strings (Figure S2B), which formed a web structure on which the smaller XR/XRW cells grew (Figure S2C,D), resulting in the clear co-localization of both strains (Figure 2C,D). In the XR–PA cultures, the web structure was clearly observable (Figures 2C and S2C), while in the XRW–PA cultures, the biofilm was so abundant that it evenly occupied the entire surface (Figures 2D and S2D).

We assessed solid–liquid interface biofilm production across all treatments in order to confirm previous reports (Figure 3A). When cultivated alone, PA produced the lowest amount of biofilm; XR and XRW produced more but there was no difference in production between the wild type and the mutant. Exposing XRW to either PA or its supernatant resulted in a significant increase in biofilm production compared to XR or XRW alone, and this increase was higher than just the sum of the individual contributions of PA and XR/XRW. An ANOVA model was applied to determine the relative variance contributions of the mutations (XR versus XRW), the presence of PA (no PA versus PA or SN), and the interaction of these two factors in determining biofilm production (Table S1). The presence of PA appeared to be the main factor explaining biofilm production (40.86% variance, $p < 0.001$), followed by the XRW mutations (32.69% variance, $p < 0.001$). However, the interaction was also significant (24.52% variance, $p < 0.001$), as biofilm production was considerably enhanced when both the mutations and PA or its supernatant were present—more than would be expected given their individual contributions.

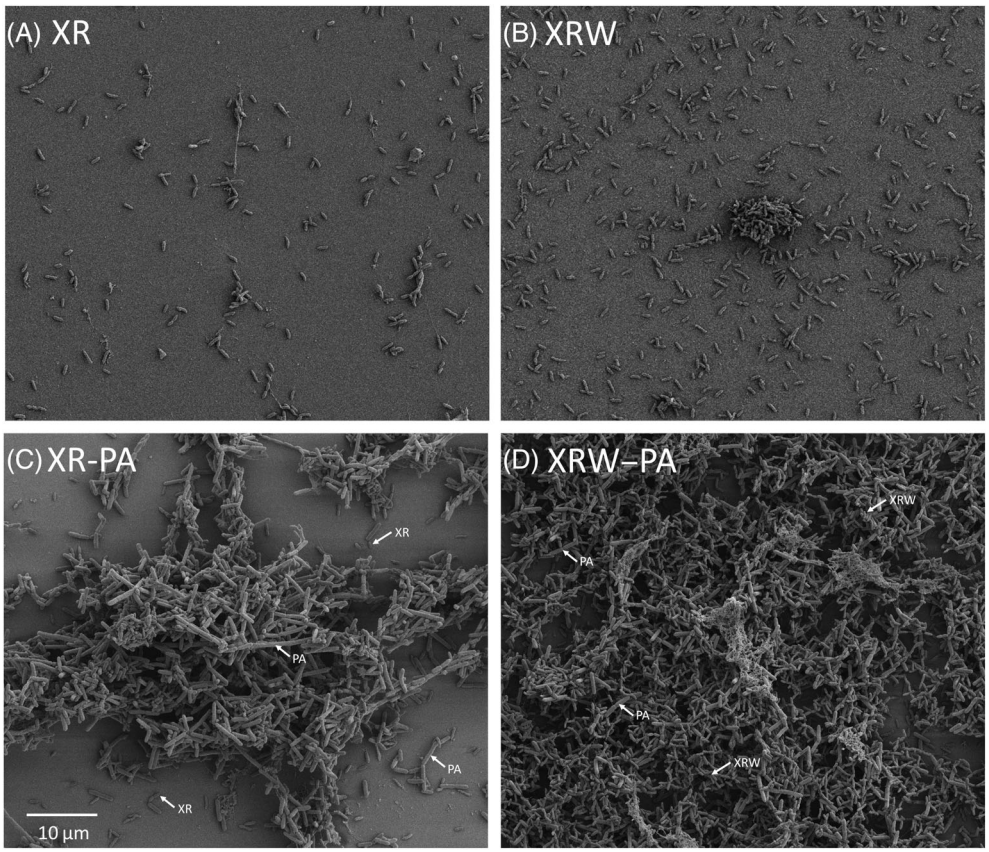

FIGURE 2 Scanning electron microscopy images of biofilms. (A) Biofilm of XR. (B) Biofilm of XRW. (C) Biofilm of XR–PA. (D) Biofilm of XRW–PA. XR/XRW cells are small, while PA cells are bigger and longer (indicated by arrows). For the purpose of comparison, images were adjusted to the same scale (scale bars = 10 µm). PA, *Paenibacillus amylolyticus*; XR, *Xanthomonas retroflexus* wild type; XRW, *Xanthomonas retroflexus* variant.

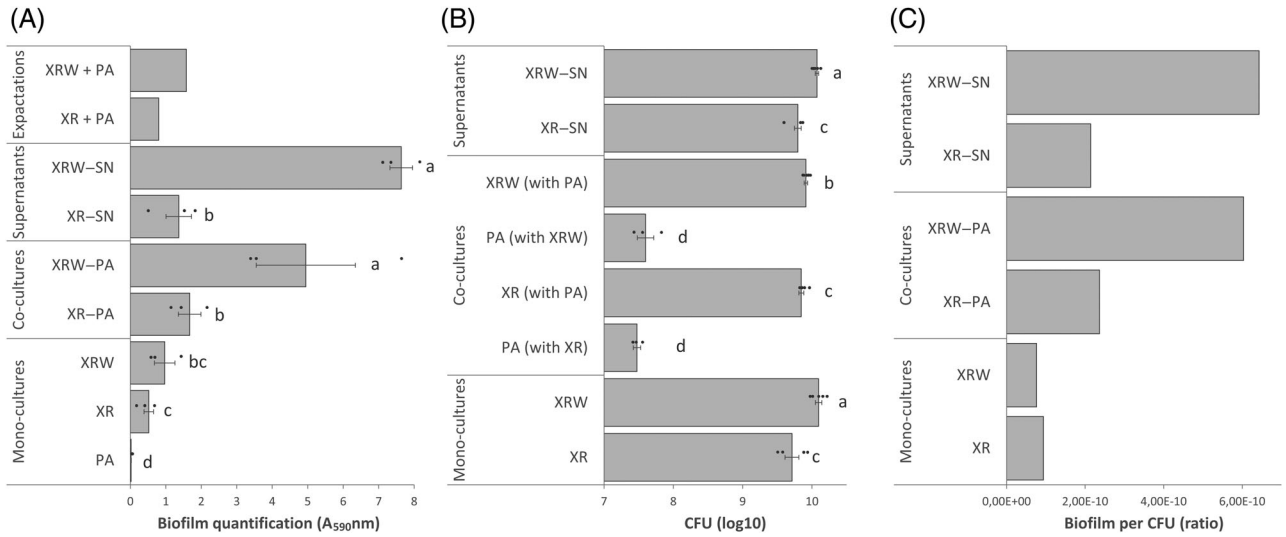

FIGURE 3 Assessment of biofilm production and colony-forming unit (CFU) counts. (A) Biofilm production in all treatments evaluated using crystal violet staining (A_{590}, $N = 3$). The expected biofilm production in co-cultures—that is, the sum of the average values for the individual strains—is given under 'expectations.' (B) CFU counts of XR, XRW and PA in all growth treatments ($N = 3$–5). PA CFUs in mono-culture biofilms were not detectable. (C) Biofilm-to-CFU ratio in all treatments, calculated from averaged crystal violet and CFU estimates obtained from panels (A) and (B). PA cell counts were not included as they were very low and did not affect the trend. Bars represent the means ± standard errors. Significance was inferred with an analysis of variance followed by a Tukey honest significant detection post hoc test ($p < 0.05$, Normality of residues verified with the d'Agostino skewedness test, $p > 0.05$). Different lower-case letters indicate significant differences. PA, *Paenibacillus amylolyticus*; SN, PA supernatant; XR, *Xanthomonas retroflexus* wild type; XRW, *Xanthomonas retroflexus* variant.

Compared to mono-cultures, CFU counts of XR were not affected by co-cultivation with PA nor its supernatant (Figure 3B). The total number of XRW CFUs was significantly higher than XR CFUs in all treatments (1.77-fold on average); this was especially true in mono-cultures (2.29-fold, $+7.17 \times 10^9$ cells) but also detectable in the co-cultures (1.16-fold, $+1.13 \times 10^9$ cells) and the supernatant treatment (1.86-fold, $+5.50 \times 10^9$ cells). Compared to the mono-culture and the supernatant treatments, CFU counts of XRW were significantly lower when co-cultured with PA (-4.52×10^9 cells). However, the negative effect of co-culture with PA did not outweigh the positive effect of the XRW mutations on its CFU counts; the net effect was still positive. PA produced the lowest CFU counts (~100-fold less than XR or XRW) and was unaffected by co-culture with XRW despite the latter's higher average number of CFUs. To compare the quantities of biofilm produced per viable XR or XRW cell recovered from the biofilm compartments, we calculated the ratio between biofilm production and the number of viable XR/XRW cells for all treatments (CV/CFU; Figure 3C). PA cell counts were marginal and thus not included for this analysis. In mono-cultures, the ratios for XR and XRW were similar, suggesting an equivalent biofilm production capacity per viable cell. In the co-culture and supernatant treatments, though, a considerable difference was noted between XR and XRW. Specifically, XRW–PA and XRW–SN had CV/CFU ratios that were 2.55- and 3.00-fold higher than those of XR–PA and XR–SN, respectively, suggesting a higher capacity for biofilm production per viable ell. Furthermore, this result was unaffected by the low CFU counts of PA.

Combined, these data document that the enhanced XRW biofilm production observed in the co-culture and supernatant treatments, was not only driven by the higher XRW cell numbers. Indeed, XRW cells in the co-culture and supernatant treatments formed larger cell aggregates and produced more biofilm per cell than those grown in mono-cultures.

Transcriptomic profiles of XR, XRW and PA

The effects of mutations on XR, XRW and PA gene expression profiles were explored among the different treatments. Our mRNA sequencing successfully retrieved 100% and 93% of CDSs in the XR and PA genomes, respectively (Figure S3). Samples from co-cultures were analysed separately, as it can be misleading to compare mRNA profiles obtained from samples containing varying numbers of genomes. First, XR and XRW profiles were compared in the mono- and supernatant cultures (Figure 4A). The mutations ($R^2 = 0.32$, $p < 0.001$), the supernatant ($R^2 = 0.29$, $p < 0.001$) and their interaction ($R^2 = 0.12$, $p < 0.001$) all had a significant influence on the transcriptomic profile of XR (PERMANOVA (permutational multivariate ANOVA), Table S2). We found that the mutations completely changed XRW expression profile compared to that of XR (first component, 42.48% variance,

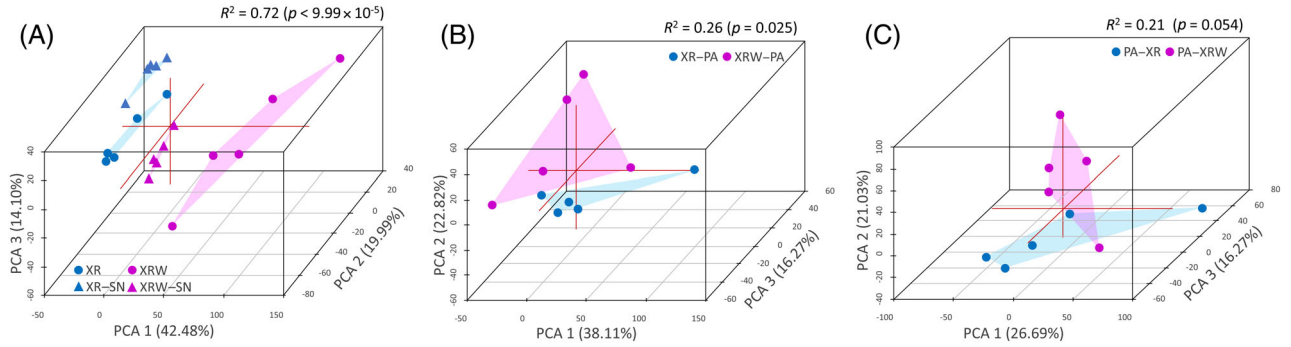

FIGURE 4 Principal component analysis (PCA) of transcriptome profiles. Panel (A) depicts the transcriptome profiles of XR (blue) and XRW (pink) grown either in mono-cultures (circles) or with PA supernatant (triangles). Panel (B) depicts the transcriptome profiles of XR (blue) and XRW (pink) in co-culture with PA. Panel (C) depicts the transcriptome profile of PA grown in co-culture either with the XR wild type (blue) or the XRW variant (pink). *R*-squared values indicate the percentage of variance explained by the PERMANOVA models (Bray–Curtis, 10,000 permutations). PA, *Paenibacillus amylolyticus*; SN, PA supernatant; XR, *Xanthomonas retroflexus* type; XRW, *Xanthomonas retroflexus* variant.

Figure 4A), and increased variations between samples (second component, 19.99% variance). Surprisingly, exposure to the PA supernatant (XRW–SN, triangles) had two main effects: (i) it partially masked the effect of mutations on XRW expression profiles, bringing them closer to those of XR mono-cultures on the first component and (ii) it greatly increased the clustering among replicates. The interaction between the supernatant and the mutations was visible on the third component (14.10% variance), which differentiated XRW–SN from XR–SN despite the masking effect. Regarding the co-culture profiles, a significant difference was detected between XR and XRW ($R^2 = 0.26$, $p = 0.025$; Table S2); XR–PA and XRW–PA clusters were close to each other but clearly distinguishable, and both featured high variation between samples (Figure 4B). With respect to PA, a marginally significant difference was detected between the transcriptomic profiles of PA–XR and PA–XRW ($R^2 = 0.214$, $p = 0.054$; Table S2), with less obvious clustering (Figure 4C).

Differentially expressed gene analysis

We extracted DEGs that explained the observed differences between XR and XRW across the three treatments (Table S3). Only expression changes that were more than twofold in magnitude were considered (FDR-adj $p < 0.01$) to exclude potential effects mediated by cell number changes (see Microscopy observations, biofilm production and fitness estimation section). Regarding the mutated genes, the change in their expression level between the treatments did not meet the twofold cut-off for being considered significant (Figure S4). Regarding PA transcriptomic profiles, no significant DEGs could be detected in PA–XRW compared to PA–XR co-cultures. However, when relaxing the filtering cut-off (FDR-adj $p < 0.05$; Table S4), we could detect three upregulated CDSs associated with the assimilatory nitrite reductase pathway and nitrite transport, an important mechanism of nitrogen acquisition. The comparison between XR and XRW profiles were in line with the multivariate analysis, as most differences were observed between the mono-cultures, where 508 DEGs across 20 functional categories were detected. In the co-culture and supernatant treatments, this number dropped to 56 DEGs across 12 functional categories and 106 DEGs across 17 functional categories, respectively. The majority of DEGs represented gene upregulation in XRW (~80%) compared to XR, with a minority representing downregulation (~20%; Table S3). The functional affiliation of DEGs, excluding those with 'unknown function and hypothetical proteins', is presented in Figure 5. Using a simple formalism, we identified 99 DEGs that were up- or downregulated in XRW as a result of the interaction between its mutations and PA supernatant (Table S5). The details on DEGs functions and filtering strategy are provided in Supporting Data 3.

In sum, the mutations in XRW led to very different expression responses depending on the presence or absence of PA or its supernatant. However, the direction and magnitude of these changes were unexpected, as the greatest number of differences was observed between XR and XRW grown in mono-cultures. Instead, the presence of PA or its supernatant masked the effects of mutations, which underscores the important role of PA in this interaction. The interaction between the effects of the mutations and those of the supernatant affected a unique set of DEGs, whose expression changes appear to promote a more-sessile lifestyle for XRW.

DISCUSSION

By investigating the mutations responsible for important phenotypic changes in microbial interactions, it may be

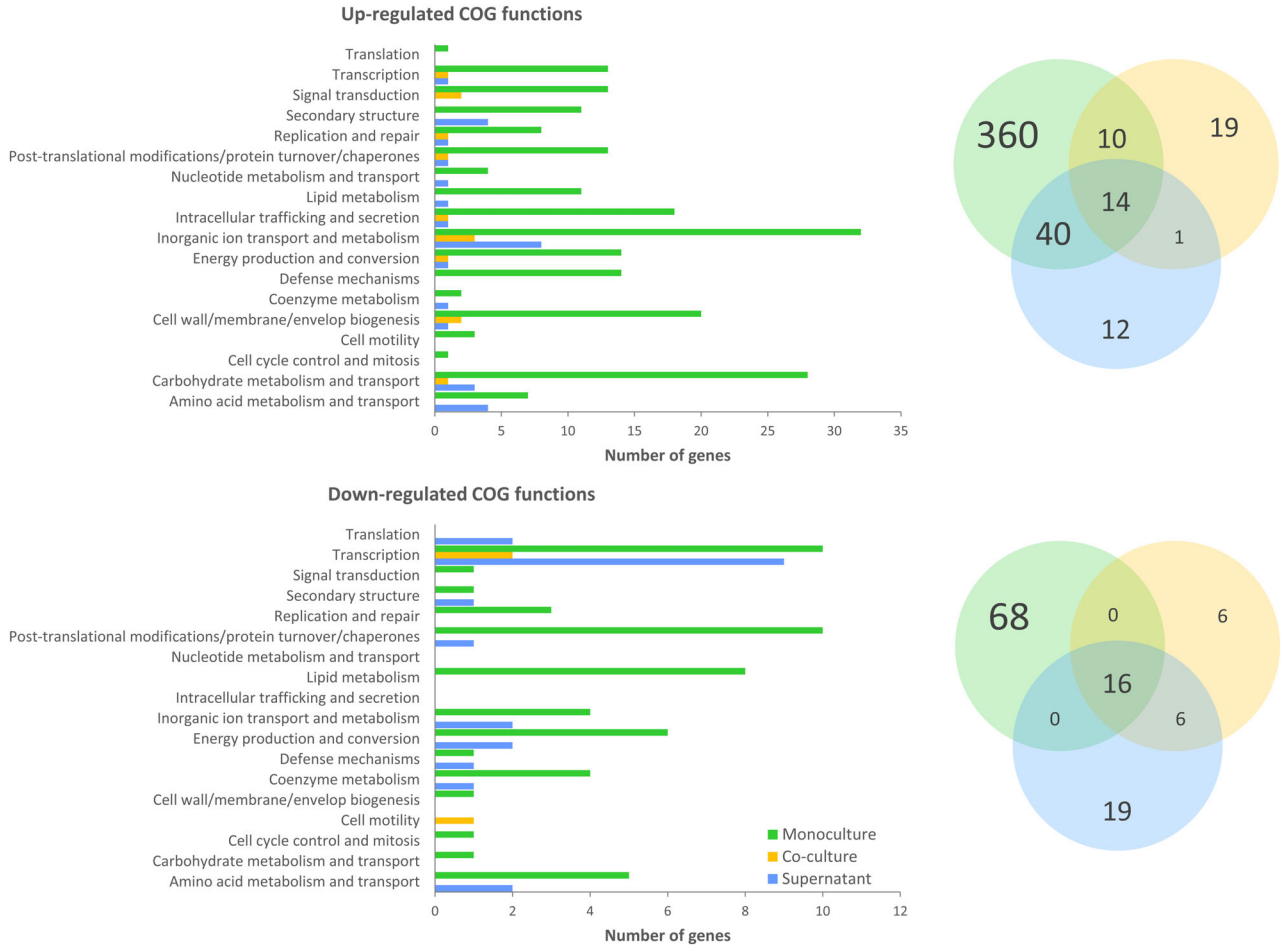

FIGURE 5 Functional classification of up- and downregulated coding DNA sequences in the *Xanthomonas retroflexus* variant compared to *X. retroflexus* in the three treatments. This figure shows only genes belonging to known functional categories. The complete list of functional assignments, including all 'unknown functions and hypothetical proteins,' is available in Table S3.

possible to shed light on how microbial interactions may evolve. Our previous work on co-cultures of the bacteria XR and PA revealed that two mutations in the genome of the former significantly increased the amount of biofilm produced (Røder et al., 2018). However, the nature of this new interaction and the mechanisms at play were unknown. Here, we hypothesised that the new phenotype was the result of an interaction between the genetic background (XRW mutations) and the biotic environmental context (presence of PA). The data presented here confirm this hypothesis, as all gathered results revealed a significant 'mutations × biotic environment' interaction in which the presence of both the mutations and PA (either directly via co-culture or indirectly via supernatant) are necessary to understand the increase in biofilm production. The fact that the effect of the supernatant was in many ways similar to that of direct co-culture with PA strongly suggests the existence of secreted molecular signals produced by PA and sensed by XR and XRW. Unexpectedly, the effect of PA on the transcriptomic profile of XRW was masking the effect of mutations. Despite this, our experimental design enabled us to detect a set of genes whose expression was related to the 'mutations × biotic environment interaction', and which may be responsible for the enhanced biofilm production observed. Our results suggest that the mutations in the XRW variant caused an overproduction of biofilm when exposed to molecular signals from PA.

Functions of mutated genes

The two mutations are located inside known domains, but away from and active sites. The response regulator peptide has features of a functional periplasmic response regulator such as PleD (Del Medico et al., 2020), which is part of a two-component regulatory system (Groisman, 2016) that uses environmental signals received by a membrane-bound histidine kinase to trigger a cellular response, notably via secondary messengers (Hughes et al., 2019). The gene is located near other genes coding peptides with known partner domains which could function as sensors or

signal transmitters to the catalytic part (e.g., HAMP in *Xanthomonas citri*; Teixeira et al., 2018). Unlike classical regulators, which are only equipped with a diguanylate cyclase domain for c-di-GMP synthesis, this regulator also has a predicted partially active phosphodiesterase 'EAL' domain for c-di-GMP degradation (Madsen et al., 2018). This implies that this regulator might have the bi-functional ability to modulate levels of c-di-GMP, which would be crucial for generating the appropriate cellular response to stimulus (Levet-Paulo et al., 2011). Three of the known functions of PleD regulators are to (i) elicit changes in cell-cycles, mediating the switch from motility to the adhering stage by correctly positioning the cell before the initiation of division (Paul et al., 2004); (ii) induce gene regulation changes (Groisman, 2016) and (iii) control c-di-GMP levels (Hughes et al., 2019). The mutation in CDS_2260 resulted in the insertion of an additional 'EAL' site, which is likely not or only weakly active. Previous mutational work on a WspR, a response regulator with a GGDEF output domain in *P. fluorescens* SBW25, revealed that mutations located around the 'GGDEF' domain in the C-terminal have important consequences on the cyclase activity (Malone et al., 2007). They also show that the activation of the regulator was linked to the disruption of the interdomain interface that release the effector-domain repression by the N-terminal receiver domain (Malone et al., 2007). This may explain the major functional repercussions on the XRW variant in mono-cultures, resulting in distinct patterns of gene upregulation, higher CFU counts and increased divisions. In contrast with previous reports from different settings (Røder et al., 2018, 2019), though, we did not observe any significant difference in biofilm production between XR and XRW mono-cultures. This may be due to the nature of the cyclase activity: to increase c-di-GMP levels and therefore biofilm production, the response regulator must first be phosphorylated by its membrane component in response to the detection of environmental cues (Malone et al., 2007; Paul et al., 2004). Small initial variations in the experimental conditions may have generated variability in the triggering level of the membrane component, thus leading to variability in biofilm production in XRW mono-cultures. With all of this in mind, the most parsimonious interpretation of the effects associated with this particular mutation is that it caused a change in conformation and/or localization of the response regulator, thus modifying its interaction with other cellular elements.

The second mutated sequence, CDS_331, encodes a cellulose biosynthesis protein that is activated by binding to c-di-GMP via two GIL domains (Fang et al., 2014); this activation by c-di-GMP results in the intense production of cellulose, an important building block of biofilms (Krasteva et al., 2017; Romling & Galperin, 2015). The gene is located in a bacterial cellulose synthesis operon of nine genes, which were all expressed in all treatments, thus indicating the potential active production of cellulose by this strain, which is an important component of biofilm (Malone et al., 2007). The mutation we identified in strain XRW substitutes an acidic and negatively charged residue (E) with a basic and positively charged one (K). The similar biofilm production between XR and XRW in mono-cultures indicates that the cellulose production capacity was likely not impaired by the mutation. As E and K are important residues for c-di-GMP binding and cycling (Düvel et al., 2016; Navarro et al., 2011), it cannot be excluded that the mutation made the protein more sensitive to c-di-GMP, which could explain the higher biofilm production in conjunction with the other mutation in the response regulator (Malone et al., 2007).

Mutations and the biotic environment

XR and XRW transcriptomes were fundamentally altered by the presence of PA. As expected, the mutation in the response regulator induced important and heterogeneous changes in gene expression of XR. Among the upregulated functions in XRW were those related to cell division, primary metabolism, iron acquisition and cell-wall biogenesis, which made sense given the higher CFU numbers and aggregation capacity observed with this strain. Conversely, most downregulated functions were linked to transcription/translation and proteolysis, which require c-di-GMP activation (Ryan, 2013). This, combined with the fact that biofilm production did not increase between XR and XRW, may suggest that the cyclase activity of the response regulator was not optimal in the mono-culture treatment. The contrast between the high sample variability in transcriptomic profiles of XRW mono-cultures and the relative sample homogeneity observed in the two other treatments emphasises the need to study the role of these mutations when PA is involved.

Surprisingly, when XRW was exposed to PA, an important masking of the mutation effects on gene regulation occurred. This result seemed counter-intuitive, but provided crucial information on the interaction between these two strains. First, the gene transcription profiles of XR and XRW were strongly influenced by the presence of PA, regardless of the mutations. This may suggests the existence of a finely tuned molecular interaction between these two naturally co-occurring strains, as previously evidenced in other studies (Herschend et al., 2017, 2018). Second, the fact that XRW biofilm production increased significantly in the supernatant treatment despite the masking effect of PA indicates that the mutated genes have an important effect on the control of biofilm synthesis. Third, the observation of a masking effect in XRW–PA implies that an unknown mechanism 'corrected' the mutation-caused changes in gene expression profiles. Despite

the masking effect, similar functions were upregulated in XRW in all treatments, with the notable exception of cell motility. Of particular interest was the upregulation of a chitin-binding protein which was reported for its implication in biofilm formation in rugose morphotypes (Shi et al., 2013). This suggests that the presence of PA favoured the sessile lifestyle of XRW while preserving its fitness advantage compared to XR. Based on our observations and data from the literature, the mutation in the response regulator appears to be the most plausible cause for the observed changes. We thus hypothesise that the masking effect could be the result of the activation (by PA signals) of the membrane-bound part of the two-component system in which the mutated response regulator is involved (Paul et al., 2004), leading to what seems to be a 'partial recovery' of its c-di-GMP synthesis function (as the masking was only noted for gene expression, not CFU counts or biofilm synthesis). However, additional analysis beyond the scope of this study would be required to verify this assertion (e.g., c-di-GMP dosage).

The possible role of PA

The mutations seemed to induce a competition effect between XRW and PA. Indeed, XRW produced more CFUs than XR in all treatments, but these counts were slightly decreased by co-culture with PA. Furthermore, specific signal transduction functions were upregulated in co-cultures (e.g., aerotaxis sensing and histidine kinase response regulators) that were indicative of sedentary competition for oxygen and an alteration in the response of XRW to the presence of PA. Both strains are able to perform anaerobic dissimilatory nitrate respiration or fermentation (Herschend et al., 2018). However, XRW seemed more affected, as PA transcriptome was barely affected by co-culturing, with the exception of the assimilatory nitrite pathway which might indicate competition for oxygen. Additional sampling of different biofilm fractions would be required to verify the link between oxygen availability and gene expression. The biosynthesis of enterobactin, a secondary structure requiring 2,3-dihydroxybenzoate, serine boundaries and isochorismatase (Gehring et al., 1997) was also up-regulated. These synthesis pathways are fundamental for siderophore synthesis and iron nutrition, especially under limiting conditions, and were found to be upregulated in both XRW exposed to PA supernatant as well as XRW mono-cultures. This result demonstrates the importance of these pathways in sustaining the enhanced growth of XRW even when PA was not involved. Sensing competitors is an important mechanism for biofilm formation (Oliveira et al., 2015), and multi-species competition has been shown to be associated with higher biofilm production in certain circumstances (Liu et al., 2019). In the present study, however, we do not have any evidence of competition between the XR wild type and PA, as CFU counts of the former were unchanged in all treatments. Furthermore, the significant decrease in XRW CFUs caused by PA was marginal compared to the gain in CFU obtained by the mutations in the co-culture treatment. In a previous study with different growth conditions, XR and PA produced significantly more cells when co-cultured, suggesting a potential mutualism between the two strains (Røder et al., 2018). Hence, the competition effect detected here is likely linked to the high growth rate and biofilm production of XRW, which would leave fewer resources available for both. Finally, the masking effect we observed in XRW gene transcription in the presence of PA could be interpreted as evidence of strong phenotypic feedback due to their co-existence in situ (the two species were co-isolated from the same environmental sample), which was proposed to be an important driver of between-species cooperation (partner-fidelity feedback and/or partner choice; Foster & Wenseleers, 2016). This could mean that, despite the negative effect of PA on XRW cell counts, these two species still interact in a similar manner in terms of gene expression, and continue to do what they are used to doing—produce biofilm—only better. The presence of PA may have changed the local environmental conditions, thus exerting a selective force that favoured the more fitted XRW variants over the XR wild type. However, although PA might have benefited from the advantages of being in a denser biofilm (Liu et al., 2019), its CFU count remained stable, in contrast with previous findings from the same strains in different settings (Røder et al., 2018). There is thus a clear need for additional work to characterise the real nature of the ecological interaction between the two strains.

Discovering the genes responding to the interaction

In this experiment, we evidenced the important role of PA on XR/XRW, as was the importance of considering the effects of mutations within their biotic context. Despite the masking effect, we successfully identified 99 genes whose expression was altered only when both the mutations and PA supernatant were present. Many were associated with the downregulation of motility and chemotaxis, making XRW even more sedentary. Instead, iron metabolism and functions related to the maintenance of the redox balance were upregulated, likely to support higher growth while reducing oxidative stress. Interestingly, the chemotaxis protein Che-Y was upregulated while the rest of the operon was not, a typical signature of the 'tumbling phenotype' (Kuo & Koshland, 1987) that is important in cell reorientation and positioning (Sidortsov et al., 2017). Cell positioning in biofilms is a crucial factor driving microbial evolution,

and plays a critical role in nutrient acquisition (Kim et al., 2014). This suggest that the cell-positioning function of XRW may be altered when exposed to PA supernatant. Furthermore, expression was also upregulated of inosine-5′-monophosphate dehydrogenase, a key enzyme in the biosynthesis of GMP (Hedstrom et al., 2011), the substrate of c-di-GMP cyclases. This indicates that the c-di-GMP production machinery was activated and suggests that the mutated response regulator has enhanced c-di-GMP production capacities when activated by PA cues, despite the negative effect of the mutation. Finally, we also detected the upregulation of several peptidases, peptidoglycan-binding proteins, and other proteins involved in outer membrane biogenesis that are important for adhesion/aggregation, cell-to-cell interaction and biofilm production (Vollmer et al., 2008). With these findings, this study makes a fundamental contribution to our understanding of how microbial interactions may evolve, as it demonstrates how the effect of mutations depends on the biotic context, leading to the expression of specific genetic functions that improved the biofilm production capacity.

CONCLUSION

Our study identified several factors that play an important role in shaping the biotic interactions between XR and PA. We found that the enhanced biofilm production by an XR mutant, which had been described in previous studies, was due to changes in the response of the mutant strain to constitutive PA cues; these involved alterations in gene regulation that affected cell positioning, aggregation and cell numbers, as well as biofilm production. Based on our observations and data from the literature, we suggest that these changes are linked to modifications in the functioning of the mutated response regulator, which has widespread effects on gene expression, notably via the upregulation of specific genes involved in the synthesis of c-di-GMP, cell positioning and biofilm synthesis. However, the fact that a large proportion of genes in this study had unknown effects highlights the need for better characterisations of gene functions in the presence of relevant environmental cues; biotic ones in particular. In such efforts, regulatory genes should receive priority, in order to shed light on the genetic dark matter that is mobilised in a diverse range of biotic and abiotic conditions. Indeed, this study reveals how mutations may lead to new genetic functions when considering the biotic environment.

AUTHOR CONTRIBUTIONS

Samuel Jacquiod: Data curation (lead); formal analysis (lead); investigation (supporting); methodology (supporting); software (equal); validation (equal); visualization (lead); writing – original draft (lead); writing – review and editing (equal). **Nanna Mee Coops Olsen:** Conceptualization (supporting); data curation (supporting); formal analysis (supporting); investigation (lead); methodology (lead); software (equal); validation (equal); visualization (supporting); writing – review and editing (equal). **Henriette Lyng Røder:** Conceptualization (supporting); data curation (supporting); formal analysis (supporting); investigation (supporting); methodology (supporting); software (equal); supervision (supporting); validation (equal); writing – review and editing (equal). **Manuel Blouin:** Formal analysis (supporting); investigation (supporting); validation (equal); writing – review and editing (equal). **Mette Burmlle:** Conceptualization (lead); data curation (supporting); funding acquisition (lead); investigation (supporting); methodology (supporting); project administration (lead); resources (lead); supervision (lead); validation (equal); writing – review and editing (equal).

ACKNOWLEDGEMENTS

Samuel Jacquiod was supported by the I-SITE Junior Fellowship BFC (RA19028.AEC.IS). The study was supported by funding from the Villum Foundation (Mette Burmølle: 10098 and 35906, Henriette Lyng Røder: 34434) and the Novo Nordic Foundation (Mette Burmølle: 27620). We would like to acknowledge the Core Facility for Integrated Microscopy in the Facility of Health and Medical Sciences, University of Copenhagen, for their support in the acquisition of the scanning electron microscopy images. The authors would also like to acknowledge Anette Løth for her technical assistance.

CONFLICT OF INTEREST STATEMENT

The authors declare that no conflicts of interest exist.

DATA AVAILABILITY STATEMENT

The mutated sequences and details of their analysis are provided in Supporting Data 1. The SEM images are provided in Supporting Data 2. The detailed analysis of DEGs is provided in Supporting Data 3. The metatranscriptomic data are available in Supporting Data 4. Other data that support this study are available as Supporting Information, or can be obtained from the corresponding author upon request. The statistical analysis was performed with the publicly available software Rgui, using publicly available function packages with referenced documentation and codes for reproducibility.

ORCID

Samuel Jacquiod https://orcid.org/0000-0002-0713-7996

REFERENCES

Aldridge, P., Paul, R., Goymer, P., Rainey, P. & Jenal, U. (2003) Role of the GGDEF regulator PleD in polar development of *Caulobacter crescentus*. *Molecular Microbiology*, 47, 1695–1708.

Barnhart, D.M., Su, S., Baccaro, B.E., Banta, L.M. & Farrand, S.F. (2013) CelR, an ortholog of the diguanylate cyclase PleD of *Caulobacter*, regulates cellulose synthesis in *Agrobacterium tumefaciens*. *Applied and Environmental Microbiology*, 79, 7188–7202.

Bar-On, Y.M. & Milo, R. (2019) Towards a quantitative view of the global ubiquity of biofilms. *Nature Reviews Microbiology*, 17, 199–200.

Boles, B.R., Thoendel, M. & Singh, P.K. (2004) Self-generated diversity produces "insurance effects" in biofilm communities. *Proceedings of the National Academy of Sciences of the United States of America*, 101, 166305.

Boratyn, G.M., Schäffer, A.A., Agarwala, R., Altschul, S.F., Lipman, D.J. & Madden, T.L. (2012) Domain enhanced lookup time accelerated BLAST. *Biology Direct*, 7, 12.

Cierra, M.I., Fort, B. & Anderson, G.G. (2022) Evaluating metabolic pathways and biofilm formation in *Stenotrophomonas maltophilia*. *Journal of Bacteriology*, 204, 1.

de Mendiburu, F. & Yaseen, M. (2020) *Agricolae: statistical procedures for agricultural research. R package version 1.4.0*. Accessed March 14th 2022. Available at: https://myaseen208.github.io/agricolae/https://cran.r-project.org/package=agricolae [Accessed 14th March 2022].

Del Medico, L., Cerletti, D., Schächle, P., Christen, M. & Christen, B. (2020) The type IV pilin PilA couples surface attachment and cell–cycle initiation in *Caulobacter crescentus*. *Proceedings of the National Academy Sciences of the United States of America*, 117, 9546–9553.

Drescher, K., Nadell, C.D., Stone, H.A., Wingreen, N.S. & Bassler, B.L. (2014) Solutions to the public goods dilemma in bacterial biofilms. *Current Biology*, 24, 50–55.

Düvel, J., Bense, S., Möller, S., Bertinetti, D., Schwede, F., Morr, M. et al. (2016) Application of synthetic peptide arrays to uncover cyclic di-GMP binding motifs. *Journal of Bacteriology*, 198, 138–146.

Fang, X., Ahmad, I., Blanka, A., Schottkowski, M., Cimdins, A., Galperin, M.Y. et al. (2014) GIL, a new c-di-GMP-binding protein domain involved in regulation of cellulose synthesis in enterobacteria. *Molecular Microbiology*, 93, 439–452.

Fiegna, F., Moreno-letelier, A., Bell, T. & Barraclough, T.G. (2015) Evolution of species interactions determines microbial community productivity in new environments. *The ISME Journal*, 9, 1235–1245.

Flemming, H.C., Wingender, J., Szewzyk, U., Steinberg, P., Rice, S.A. & Kjelleberg, S. (2016) Biofilms: an emergent form of bacterial life. *Nature Reviews Microbiology*, 14, 563–575.

Foster, K.R. & Wenseleers, T. (2016) A general model for the evolution of mutualisms. *Journal of Evolutionary Biology*, 19, 1283–1293.

Futuyma, D.J. (2010) How species affect each other's evolution. *Evolution: Education and Outreach*, 3, 3–5.

Gehring, A.M., Bradley, K.A. & Walsh, C.T. (1997) Enterobactin biosynthesis in *Escherichia coli*: isochorismate lyase (EntB) is a bifunctional enzyme that is phosphopantetheinylated by EntD and then acylated by EntE using ATP and 2,3-dihydroxybenzoate. *Biochemistry*, 36, 8495–8503.

Groisman, E.A. (2016) Feedback control of two-component regulatory systems. *Annual Review of Microbiology*, 70, 103–124.

Hansen, S.K., Rainey, P.B., Janus, A.J., Haagensen, J.A.J. & Molin, S. (2007) Evolution of species interactions in a biofilm community. *Nature*, 445, 533–536.

Hansen, L.B.S., Ren, D., Burmølle, M. & Sørensen, S.J. (2017) Distinct gene expression profile of *Xanthomonas retroflexus* engaged in synergistic multispecies biofilm formation. *The ISME Journal*, 1, 300–303.

Hedstrom, L., Liechti, G., Goldberg, J.B. & Gollapalli, D.R. (2011) The antibiotic potential of prokaryotic IMP dehydrogenase inhibitors. *Current Medicinal Chemistry*, 18, 1909–1918.

Herschend, J., Damholt, Z.B.V., Marquard, A.M., Svensson, B., Søren, J.S., Hägglund, P. et al. (2017) A meta-proteomics approach to study the interspecies interactions affecting microbial biofilm development in a model community. *Scientific Reports*, 7, 16483.

Herschend, J., Koren, K., Røder, H.L., Brejnrod, A., Kühl, M. & Burmølle, M. (2018) In vitro community synergy between bacterial soil isolates can be facilitated by pH stabilization of the environment. *Applied and Environmental Microbiology*, 84, 21.

Huerta-Cepas, J., Szklarczyk, D., Forslund, K., Cook, H., Heller, D., Walter, M.C. et al. (2016) eggNOG 4.5: a hierarchical orthology framework with improved functional annotations for eukaryotic, prokaryotic and viral sequences. *Nucleic Acids Research*, 44, D286–D293.

Hughes, E.D., Byrne, B.G. & Swanson, M.S. (2019) A two-component system that modulates cyclic di-GMP metabolism promotes *Legionella pneumophila* differentiation and viability in low-nutrient conditions. *Journal of Bacteriology*, 201, e00253-19.

Jacquiod, S., Demanèche, S., Franqueville, L., Ausec, L., Xu, Z., Delmont, T.O. et al. (2014) Characterization of new bacterial catabolic genes and mobile genetic elements by high throughput genetic screening of a soil metagenomic library. *Journal of Biotechnology*, 190, 18–29.

Kim, W., Racimo, F., Schluter, J., Stuart, B., Levy, S.B. & Foster, K.R. (2014) Importance of positioning for microbial evolution. *Proceedings of the National Academy of Sciences of the United States of America*, 111, E1639–E1647.

Kopylova, E., Noé, L. & Touzet, H. (2012) SortMeRNA: fast and accurate filtering of ribosomal RNAs in metatranscriptomic data. *Bioinformatics*, 28, 3211–3217.

Krasteva, P.V., Bernal-Bayard, J., Travier, L., Martin, F.A., Kaminski, P.A., Karimova, G. et al. (2017) Insights into the structure and assembly of a bacterial cellulose secretion system. *Nature Communications*, 8, 2065.

Kumari, U.M., Kumari, S. & Das, S. (2022) Unraveling the complex regulatory networks in biofilm formation in bacteria and relevance of biofilms in environmental remediation. *Critical Reviews in Biochemistry and Molecular Biology*, 57, 3305–3332.

Kuo, S.C. & Koshland, D.E. (1987) Roles of cheY and cheZ gene products in controlling flagellar rotation in bacterial chemotaxis of *Escherichia coli*. *Journal of Bacteriology*, 169, 1307–1314.

Langmead, B. & Salzberg, S.L. (2012) Fast gapped-read alignment with Bowtie 2. *Nature Methods*, 9, 357–359.

Lee, K.W.K., Periasamy, S., Mukherjee, M., Xie, C., Kjelleberg, S. & Rice, S.A. (2014) Biofilm development and enhanced stress resistance of a model, mixed-species community biofilm. *The ISME Journal*, 8, 894–907.

Lenski, R.E. (2017) Experimental evolution and the dynamics of adaptation and genome evolution in microbial populations. *The ISME Journal*, 11, 2181–2194.

Levet-Paulo, M., Lazzaroni, J.C., Gilbert, C., Atlan, D., Doublet, P. & Vianney, A. (2011) The atypical two-component sensor kinase Lpl0330 from *Legionella pneumophila* controls the bifunctional diguanylate cyclase-phosphodiesterase Lpl0329 to modulate bis-(3′-5′)-cyclic dimeric GMP synthesis. *The Journal of Biological Chemistry*, 286, 31136–31144.

Liao, Y., Smyth, G.K. & Shi, W. (2014) featureCounts: an efficient general purpose program for assigning sequence reads to genomic features. *Bioinformatics*, 30, 923–930.

Liu, W., Jacquiod, S., Brejnrod, A., Russel, J., Burmølle, M. & Sørensen, S.J. (2019) Deciphering links between bacterial interactions and spatial organization in multispecies biofilms. *The ISME Journal*, 13, 3054–3066.

Madsen, J.S., Hylling, O., Jacquiod, S., Pécastaings, S., Hansen, L.H., Riber, L. et al. (2018) An intriguing relationship between the cyclic diguanylate signaling system and horizontal gene transfer. *The ISME Journal*, 12, 2330–2334.

Madsen, J.S., Røder, H.L., Russel, J., Sørensen, H., Burmølle, M. & Sørensen, S.J. (2016) Coexistence facilitates interspecific

biofilm formation in complex microbial communities. *Environmental Microbiology*, 18, 2565–2574.
Malone, J.D., Williams, R., Christen, M., Jenal, U., Spiers, A.J. & Rainey, P.B. (2007) The structure–function relationship of WspR, a *Pseudomonas fluorescens* response regulator with a GGDEF output domain. *Microbiology*, 153, 980–994.
McDonald, M.J. (2019) Microbial experimental evolution – a proving ground for evolutionary theory and a tool for discovery. *EMBO Reports*, 20, e46992.
Nasipuri, P., Herschend, J., Brejnrod, A.D., Madsen, J.S., Espersen, R., Svensson, B. et al. (2020) Community-intrinsic properties enhance keratin degradation from bacterial consortia. *PLoS One*, 15, e0228108.
Navarro, M.V.A.S., Newell, P.D., Krasteva, P.V., Chatterjee, D., Madden, D.R., O'Toole, G.A. et al. (2011) Structural basis for c-di-GMP-mediated inside-out signaling controlling periplasmic proteolysis. *PLoS Biology*, 9, e1000588.
Nielsen, H. (2017) Predicting secretory proteins with SignalP. In: Kihara, D. (Ed.) *Protein function prediction (Methods in Molecular Biology)*, Vol. 1611. New York: Humana Press, pp. 59–73.
Oksanen, J., Blanchet, F.G., Friendly, M., Kindt, R., Legendre, P., McGlinn, D. et al. (2020) *Vegan: community ecology package. R package version 2.5-7*. Available at: https://CRAN.R-project.org/package=vegan [Accessed 14th March 2022].
Oliveira, N.M., Martinez-Garcia, E., Xavier, J., Durham, W.M., Kolter, R., Kim, W. et al. (2015) Biofilm formation as a response to ecological competition. *PLoS Biology*, 13, e1002191.
O'Toole, G.A. (2011) Microtiter dish biofilm formation assay. *Journal of Visualized Experiments*, 30, 2437.
Overbeek, R., Olson, R., Pusch, G.D., Olsen, G.J., Davis, J.J., Disz, T. et al. (2014) The SEED and the rapid annotation of microbial genomes using subsystems technology (RAST). *Nucleic Acids Research*, 42, D206–D214.
Paul, R., Weiser, S., Amiot, N.C., Chan, C., Schirmer, T., Giese, B. et al. (2004) Cell cycle-dependent dynamic localization of a bacterial response regulator with a novel di-guanylate cyclase output domain. *Genes & Development*, 18, 715–727.
Poltak, S. & Cooper, V. (2011) Ecological succession in long-term experimentally evolved biofilms produces synergistic communities. *The ISME Journal*, 5, 369–378.
R Core Team. (2020) *R: a language and environment for statistical computing*. Vienna: R Foundation for Statistical Computing. Available at: http://www.R-project.org/
Raghupathi, P.K., Liu, W., Sabbe, K., Houf, K., Burmølle, M. & Sørensen, S.J. (2018) Synergistic interactions within a multispecies biofilm enhance individual species protection against grazing by a pelagic protozoan. *Frontiers in Microbiology*, 8, 2649.
Ren, D., Madsen, J.S., de la Cruz-Perera, C.I., Bergmark, L., Sørensen, S.J. & Burmølle, M. (2014) High-throughput screening of multispecies biofilm formation and quantitative PCR-based assessment of individual species proportions, useful for exploring interspecific bacterial interactions. *Microbial Ecology*, 68, 146–154.
Ren, D., Madsen, J.S., Sørensen, S.J. & Burmølle, M. (2015) High prevalence of biofilm synergy among bacterial soil isolates in cocultures indicates bacterial interspecific cooperation. *The ISME Journal*, 9, 81–89.
Richter, A., Hölscher, T., Pausch, P., Sehrt, T., Brockhaus, F., Bange, G. et al. (2018) Hampered motility promotes the evolution of wrinkly phenotype in *Bacillus subtilis*. *BMC Evolutionary Biology*, 18, 155.
Robinson, M.D., McCarthy, D.J. & Smyth, G.K. (2010) edgeR: a bioconductor package for differential expression analysis of digital gene expression data. *Bioinformatics*, 26, 139–140.
Røder, H.L., Herschend, J., Russel, J., Andersen, M.F., Madsen, J.S., Sørensen, S.J. et al. (2018) Enhanced bacterial mutualism through an evolved biofilm phenotype. *The ISME Journal*, 12, 2608–2618.
Røder, H.L., Liu, W., Sørensen, J.S., Madsen, J.S. & Burmølle, M. (2019) Interspecies interactions reduce selection for a biofilm-optimized variant in a four-species biofilm model. *Environmental Microbiology Reports*, 11, 835–839.
Røder, H.L., Sørensen, S.J. & Burmølle, M. (2016) Studying bacterial multispecies biofilms: where to start? *Trends in Microbiology*, 24, 503–513.
Romling, U. & Galperin, M.Y. (2015) Bacterial cellulose biosynthesis: diversity of operons, subunits, products, and functions. *Trends in Microbiology*, 23, 545–557.
Ryan, R.P. (2013) Cyclic di-GMP signalling and the regulation of bacterial virulence. *Microbiology*, 159, 1286–1297.
Scheuerl, T., Hopkins, M., Nowell, R.W., Rivett, D.W., Barraclough, T.G. & Bell, T. (2020) Bacterial adaptation is constrained in complex communities. *Nature Communications*, 11, 754.
Shi, M., Wu, L., Xia, Y., Chen, H., Luo, Q., Sun, L. et al. (2013) Exoprotein production correlates with morphotype changes of nonmotile *Shewanella oneidensis* mutants. *Journal of Bacteriology*, 195(1), 463–1474.
Sidortsov, M., Yakov, M. & Avraham, B. (2017) Role of tumbling in bacterial swarming. *Physical Review E*, 96, 022407.
Spiers, A.J., Bohannon, J., Gehrig, S.M. & Rainey, P.B. (2003) Biofilm formation at the air-liquid interface by the *Pseudomonas fluorescens* SBW25 wrinkly spreader requires an acetylated form of cellulose. *Molecular Microbiology*, 50, 15–27.
Spiers, A.J. & Rainey, P.B. (2005) The *Pseudomonas fluorescens* SBW25 wrinkly spreader biofilm requires attachment factor, cellulose fibre and LPS interactions to maintain strength and integrity. *Microbiology*, 151, 2829–2839.
Teixeira, R.D., Guzzo, C.R., Arévalo, S.J., Andrade, M.O., Abrahão, J., de Souza, R.F. et al. (2018) A bipartite periplasmic receptor–diguanylate cyclase pair (XAC2383–XAC2382) in the bacterium *Xanthomonas citri*. *The Journal of Biological Chemistry*, 293, 10767–10781.
Thompson, J.N. (1999) The evolution of species interactions. *Science*, 284(5423), 2116–2118.
Udall, Y.C., Deeni, Y., Hapca, S.M., Raikes, D. & Spiers, A.J. (2015) The evolution of biofilm-forming wrinkly spreaders in static microcosms and drip-fed columns selects for subtle differences in wrinkleality and fitness. *FEMS Microbiology Ecology*, 91, 57.
Valentini, M. & Filloux, A. (2016) Biofilms and cyclic di-GMP (c-di-GMP) signaling: lessons from *Pseudomonas aeruginosa* and other bacteria. *The Journal of Biological Chemistry*, 291, 12547–12555.
Vollmer, W., Joris, B., Charlier, P. & Foster, S. (2008) Bacterial peptidoglycan (murein) hydrolases. *FEMS Microbiology Reviews*, 32, 259–286.
Williams, H.T.P. & Lenton, T.M. (2007) Artificial selection of simulated microbial ecosystems. *Proceedings of the National Academy of Sciences of the United States of America*, 104, 8918–8923.
Yang, N., Nesme, J., Røder, H.L., Li, X., Zuo, Z., Petersen, M. et al. (2021) Emergent bacterial community properties induce enhanced drought tolerance in *Arabidopsis*. *Npj Biofilms and Microbiomes*, 7, 82.

SUPPORTING INFORMATION

Additional supporting information can be found online in the Supporting Information section at the end of this article.

How to cite this article: Jacquiod, S., Olsen, N.M.C., Blouin, M., Røder, H.L. & Burmølle, M. (2023) Genotypic variations and interspecific interactions modify gene expression and biofilm formation of *Xanthomonas retroflexus*. *Environmental Microbiology*, 1–14. Available from: https://doi.org/10.1111/1462-2920.16503